

**Argonne National Laboratory**

**A WIDE-BAND CHARGE-SENSITIVE  
PREAMPLIFIER FOR PROTON-RECOIL  
PROPORTIONAL COUNTING**

by

J. M. Larson

The facilities of Argonne National Laboratory are owned by the United States Government. Under the terms of a contract (W-31-109-Eng-38) between the U. S. Atomic Energy Commission, Argonne Universities Association and The University of Chicago, the University employs the staff and operates the Laboratory in accordance with policies and programs formulated, approved and reviewed by the Association.

#### MEMBERS OF ARGONNE UNIVERSITIES ASSOCIATION

The University of Arizona  
Carnegie-Mellon University  
Case Western Reserve University  
The University of Chicago  
University of Cincinnati  
Illinois Institute of Technology  
University of Illinois  
Indiana University  
Iowa State University  
The University of Iowa

Kansas State University  
The University of Kansas  
Loyola University  
Marquette University  
Michigan State University  
The University of Michigan  
University of Minnesota  
University of Missouri  
Northwestern University  
University of Notre Dame

The Ohio State University  
Ohio University  
The Pennsylvania State University  
Purdue University  
Saint Louis University  
Southern Illinois University  
University of Texas  
Washington University  
Wayne State University  
The University of Wisconsin

#### LEGAL NOTICE

This report was prepared as an account of Government sponsored work. Neither the United States, nor the Commission, nor any person acting on behalf of the Commission:

A. Makes any warranty or representation, expressed or implied, with respect to the accuracy, completeness, or usefulness of the information contained in this report, or that the use of any information, apparatus, method, or process disclosed in this report may not infringe privately owned rights; or

B. Assumes any liabilities with respect to the use of, or for damages resulting from the use of any information, apparatus, method, or process disclosed in this report.

As used in the above, "person acting on behalf of the Commission" includes any employee or contractor of the Commission, or employee of such contractor, to the extent that such employee or contractor of the Commission, or employee of such contractor prepares, disseminates, or provides access to, any information pursuant to his employment or contract with the Commission, or his employment with such contractor.

Printed in the United States of America  
Available from

Clearinghouse for Federal Scientific and Technical Information  
National Bureau of Standards, U. S. Department of Commerce  
Springfield, Virginia 22151

Price: Printed Copy \$3.00; Microfiche \$0.65

ARGONNE NATIONAL LABORATORY  
9700 South Cass Avenue  
Argonne, Illinois 60439

A WIDE-BAND CHARGE-SENSITIVE  
PREAMPLIFIER FOR PROTON-RECOIL  
PROPORTIONAL COUNTING

by

J. M. Larson

Reactor Physics Division

February 1969



## TABLE OF CONTENTS

	<u>Page</u>
ABSTRACT . . . . .	4
INTRODUCTION. . . . .	4
GENERAL CIRCUIT DESCRIPTION . . . . .	5
PREAMPLIFIER SATURATION. . . . .	7
NOISE CHARACTERISTICS . . . . .	9
PREAMPLIFIER OUTPUT RESPONSE . . . . .	12
PREAMPLIFIER CONSTRUCTION. . . . .	12
CONNECTION TO THE PROPORTIONAL COUNTER. . . . .	12
FURTHER APPLICATIONS . . . . .	15
APPENDIX--Overload Pulse Width . . . . .	16
REFERENCES . . . . .	18



## LIST OF FIGURES

<u>No.</u>	<u>Title</u>	<u>Page</u>
1.	Preamplifier Schematic Diagram . . . . .	6
2.	Pulse Profiles. . . . .	7
3.	Plot of Overload Pulse Width . . . . .	9
4.	Preamplifier Response . . . . .	13
5.	Photograph of Preamplifier . . . . .	14

## TABLE

<u>No.</u>	<u>Title</u>	<u>Page</u>
I.	Equivalent Input Noise Charge as a Function of External Input Capacitance and Shaping Time Constants . . . . .	11





# A WIDE-BAND CHARGE-SENSITIVE PREAMPLIFIER FOR PROTON-RECOIL PROPORTIONAL COUNTING

by

J. M. Larson

## ABSTRACT

This report describes a solid-state charge-sensitive preamplifier for use with proportional counters in proton-recoil spectrometers. The preamplifier has a charge gain of  $2 \times 10^{12}$  V/coulomb and exhibits a rise time of 15 nsec, without overshoot, with 10 pF of external input capacity. A high-transconductance field-effect transistor is used in the input stage and near theoretical noise performance is obtained. The circuit is direct-coupled and is compatible with pole-zero compensated amplifier systems. The preamplifier features a 20-V peak output swing to allow high count-rate capability and the amplification of extreme overloads without saturation.

## INTRODUCTION

The amplifiers used in proton-recoil spectrometers of the type described by Bennett<sup>1</sup> are subjected to severe overloads when the proportional counters are operated at high gas multiplication. These overloads can create lengthy dead times in the shaping amplifiers of the spectrometer, thus limiting, to relatively low levels, the maximum counting rates that can be accepted without introducing distortion.

Pole-zero cancellation techniques<sup>2</sup> may be used in systems of this type to improve overload response and thus minimize dead time. However, if pole-zero cancellation is to be used effectively, the preamplifier used with the system must have (1) an output pulse that decays exponentially with a single time constant, and (2) a large output swing such that preamplifier saturation does not occur.

In addition, a preamplifier to be used for proton-recoil proportional counting must have fast rise time, exhibit low noise, and be physically small so it can be mounted near the proportional counter with minimum perturbation of the neutron spectrum being measured.



This report describes a preamplifier that has been designed to be compatible with pole-zero compensated amplifier systems, but that also exhibits the low noise, fast rise time, and small physical dimensions required for proton-recoil proportional counting. The preamplifier features a 20-V peak output swing, which allows it to accept large overloads at high counting rates without saturation.

## GENERAL CIRCUIT DESCRIPTION

The preamplifier circuit is shown schematically in Fig. 1. The circuit is a charge-sensitive configuration using a Texas Instruments SFB-8558 field-effect transistor (FET),  $Q_1$  in the first stage. Transistors  $Q_2$  and  $Q_3$  are cascode-connected. Transistor  $Q_4$  is a current source whose output impedance, in parallel with the output impedance of  $Q_3$  and the input impedance of  $Q_5$ , comprises the collector load impedance of  $Q_3$ .<sup>\*</sup> Transistor  $Q_5$  is an emitter follower that drives the complementary emitter follower consisting of  $Q_6$  and  $Q_7$ . Capacitor  $C_f$  and resistor  $R_f$  are the feedback elements of the charge loop.

The open-loop gain,  $A_{OL}$ , of the circuit may be expressed as  $A_{OL} \cong g_m Z_L$ , where

$g_m$  = the transconductance of the input FET,

$Z_L$  = the parallel combination of the output impedance of  $Q_3$ ,  $Q_4$ , and the input impedance ( $Z_{in}$ ) of  $Q_5$ ,

and

$Z_L \cong Z_{in}$  of  $Q_5$ .

The typical transconductance of the SFB-8558 is approximately  $22 \times 10^{-3}$  mho, and in this circuit  $Z_L \cong 500$  k $\Omega$  minimum. This results in a typical open-loop gain of approximately 10,000.

The base of  $Q_3$  and the collectors of  $Q_5$  and  $Q_6$  are connected to +24 V. This allows the preamplifier output, at the junction of the emitter resistors of  $Q_6$  and  $Q_7$ , to swing to +20 V when the preamplifier is driving a terminated 93  $\Omega$  coaxial cable.

Diode CR1 is normally reverse-biased and protects the base emitter junction of  $Q_3$  in the event of a power-supply failure or transient condition causing the saturation of  $Q_2$ .

<sup>\*</sup>This technique is used in the Tennelec TC-135 preamplifier.

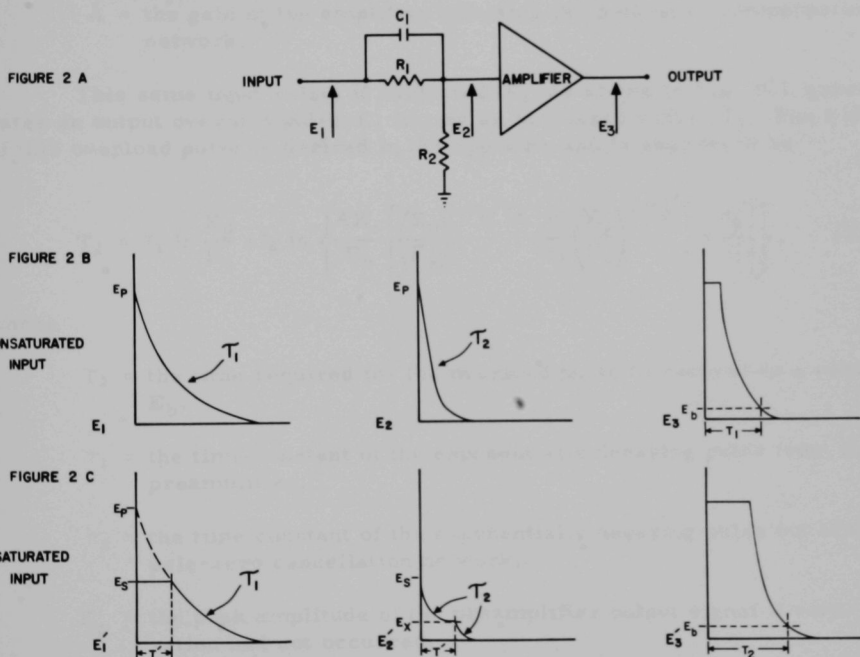






# PREAMPLIFIER SATURATION

In proton-recoil systems, measurements must often be made when the proportional counters are operated with gas multiplications of 4000 and greater. This mode of operation generates large overloads (some particles depositing a charge of greater than  $15 \times 10^{-12}$  coulombs in the detector) and may result in preamplifier saturation. Preamplifier saturation is undesirable as it increases the width of the corresponding overload pulses in the shaping amplifiers following the preamplifier and thus reduces the count-rate capabilities of the overall system. The effect of saturation is shown in Fig. 2, where a saturated and an unsaturated pulse from a preamplifier are passed through a pole-zero correction network and then are amplified by an amplitude-limiting amplifier.



ID-103-11921

Fig. 2. Pulse Profiles

The width of the overload pulse  $E_3$  due to the unsaturated input  $E_1$  (as shown in Fig. 2B) is readily determined to be

$$T_1 = \tau_2 \ln (E_p A / E_b), \quad (1)$$





where

$T_1$  = the time for the overload pulse to recover to a voltage  $E_b$ ,

$\tau_2$  = the time constant of the exponentially decaying pulse out of the pole-zero cancellation network,

$E_p$  = the peak amplitude of the preamplifier output signal,

$E_b$  = the reference level to which the overload decays,

and

$A$  = the gain of the amplifier following the pole-zero compensation network.

This same input pulse, if saturated ( $E_1'$ , as shown in Fig. 2C), generates an output overload pulse  $E_3'$  having an increased width,  $T_2$ . The width of this overload pulse is derived in the appendix and is expressed as

$$T_2 = \tau_1 \ln \frac{E_p}{E_s} + \tau_2 \ln \left\{ \frac{AE_s}{E_b} \left[ \left( \frac{E_p}{E_s} \right)^{-\tau_1/\tau_2} - \frac{\tau_2}{\tau_1} \left( \frac{E_p}{E_s} \right)^{-\tau_1/\tau_2} + \frac{\tau_2}{\tau_1} \right] \right\}, \quad (2)$$

where

$T_2$  = the time required for the overload pulse to recover to a voltage  $E_b$ ,

$\tau_1$  = the time constant of the exponentially decaying pulse from the preamplifier,

$\tau_2$  = the time constant of the exponentially decaying pulse out of the pole-zero cancellation network,

$E_p$  = the peak amplitude of the preamplifier output signal if saturation had not occurred,

$E_s$  = the saturated level of the preamplifier output pulse,

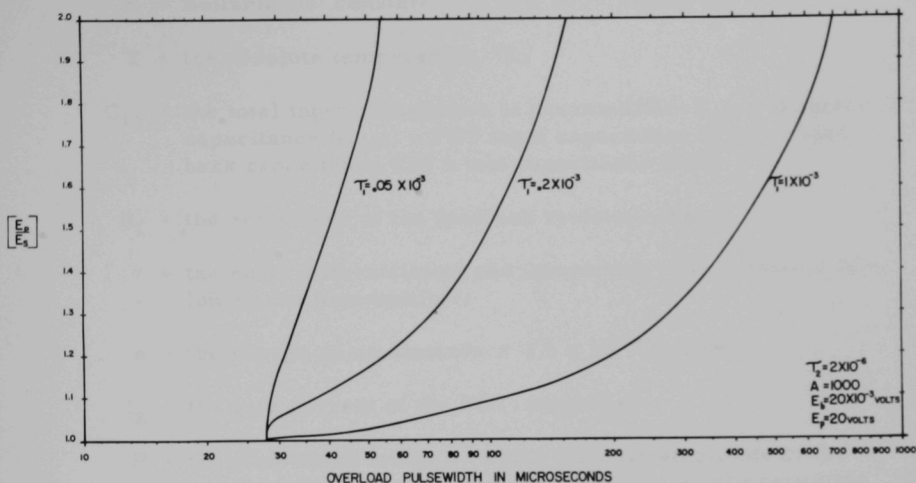
$E_b$  = the reference level to which the overload decays,

and

$A$  = the gain of the amplifier following the pole-zero compensation network.



Figure 3 is a plot of  $T_2$  as a function of  $\tau_1$  and  $E_p/E_s$ . In this plot, it is assumed that  $E_p = 20$  V,  $E_b = 20 \times 10^{-3}$  V,  $A = 10^3$ , and  $\tau_2 = 2 \times 10^{-6}$  sec. Separate curves are plotted for  $\tau_1 = 10^{-3}$  sec,  $\tau_1 = 0.2 \times 10^{-3}$  sec, and  $\tau_1 = 0.05 \times 10^{-3}$  sec.



ID-103-11920

Fig. 3. Plot of Overload Pulse Width

As can be noted from Fig. 3, the overload pulse width from the linear amplifier is increased if the preamplifier saturates, the increase being magnified when the differentiating time constant of the preamplifier is large. To avoid saturation, a preamplifier output swing of about 20 V or greater was desired. In addition, a relatively short preamplifier differentiating time constant was also wanted to minimize the overload pulse width from the linear amplifier if some saturation in the preamplifier did occur. In this application, a preamplifier differentiating time constant of about 500  $\mu$ sec was felt to be about the minimum that could be used because of the increase in preamplifier noise that accompanies a decrease in this time constant.

### NOISE CHARACTERISTICS

The equivalent input noise charge of the preamplifier, neglecting flicker effects in the FET ( $Q_1$ ), may be expressed as<sup>3,4</sup>

$$(\text{ENC})^2 = \frac{\frac{KTR_n(C_{in})^2}{2\tau} + \frac{eI_g\tau}{4} + \frac{KT\tau}{2R_f}}{P^2} \quad (3)$$



where

ENC = equivalent input noise charge in rms coulombs;

$K$  = Boltzmann's constant =  $1.37 \times 10^{-23}$  joules/°K;

$T$  = the absolute temperature, °K;

$C_{in}$  = the total input capacitance of preamplifier;  $C_{in}$  = detector capacitance ( $C_{det}$ ) + FET input capacitance ( $C_{iss}$ ) + feedback capacitance ( $C_f$ ) + test capacitance ( $C_T$ );

$R_f$  = the resistance of the feedback resistor, ohms;

$\tau$  = the equal differentiating and integrating time constants following the preamplifier;

$e$  = the charge on an electron =  $1.6 \times 10^{-19}$  coulomb;

$I_g$  = the gate current of the FET, amperes;

$P$  = the attenuation factor by which the peak amplitude of the preamplifier output pulse is reduced by the differentiating and integrating time constants of the shaping amplifiers;  
 $P = 0.37$  when the shaping time constants are equal;<sup>4</sup>

and

$R_n$  = the equivalent noise resistance of the input FET;  
 $R_n \cong 0.7/g_m$ .<sup>5</sup>

There are two noise regions of interest in this application. The first is the region determined by the differentiating and integrating time constants of the low-frequency shaping amplifier. These time constants are normally equal and are set between 1 and 2  $\mu$ sec. The effective input noise charge over this region is defined by Eq. 3.

The second region of interest is the spectrum of frequencies that must be amplified to determine the rate of rise of the output pulse from the preamplifier. This region is bounded by the upper limits of the bandwidth of the preamplifier and by the relatively short time constant of the differentiating network (20-100 nsec) in the fast amplifier following the preamplifier. At these frequencies, the noise contribution from the feedback resistor  $R_f$  and from the FET gate current is negligible. The equivalent input noise charge is then due almost totally to the equivalent noise resistance of the input FET and may be expressed as<sup>3</sup>



$$(\text{ENC})^2 \cong \frac{KTR_n \tau_1 C_{in}^2}{\tau_2 P^2 (\tau_1 + \tau_2)}, \quad (4)$$

where

$\tau_1$  = the differentiating time constant of the shaping amplifier,

and

$\tau_2$  = the integrating time constant of the shaping amplifier.

If no integration is used following the preamplifier,  $\tau_2 \cong t_r/2.2$ , where  $t_r$  is the 10-90% rise time of the preamplifier output.

When  $\tau_1 = \tau_2 = \tau$  and  $t_r/2.2 \ll \tau$ , Eq. 4 reduces to

$$(\text{ENC})^2 \cong \frac{KTR_n C_{in}^2}{2\tau P^2}. \quad (5)$$

The noise generated by the preamplifier at the low and high frequencies may be readily computed, once all the circuit parameters are known. In this case, the parameters are  $g_m \cong 22 \times 10^{-3}$  mho,  $R_f = 1 \times 10^9 \Omega$ ,  $C_f = 0.5$  pF,  $I_g \cong 0.3 \times 10^{-9}$  A,  $C_{det} \cong 10$  pF,  $C_{iss} \cong 15$  pF, and  $C_T = 0.5$  pF.

The preamplifier theoretical noise has been calculated (using the parameters noted above and Eqs. 3 and 5 for equal shaping time constants of 2  $\mu$ sec and 100 nsec. The results of these calculations are tabulated in Table I.

TABLE I. Equivalent Input Noise Charge as a Function of External Input Capacitance and Shaping Time Constants

External Input Capacitance, pF	Calculated Noise, rms coulombs		Measured Noise, rms coulombs	
	$\tau = 2 \mu\text{sec}$	$\tau = 100 \text{ nsec}$	$\tau = 2 \mu\text{sec}$	$\tau = 100 \text{ nsec}$
0	$16 \times 10^{-18}$	$36 \times 10^{-18}$	$21 \times 10^{-18}$	$42 \times 10^{-18}$
10	$21 \times 10^{-18}$	$58 \times 10^{-18}$	$26 \times 10^{-18}$	$60 \times 10^{-18}$

Comparative noise measurements using a Ballantine 323 rms voltmeter were made for the same time constants; these measurements are also tabulated in Table I. The external input capacitance and the transconductance and input capacitance of the FET were measured to





within 5% of the values used in the theoretical calculations. As can be noted from Table I, close agreement was obtained between measured and calculated noise.

### PREAMPLIFIER OUTPUT RESPONSE

A relatively high charge gain was desired in this preamplifier to minimize the noise contribution of following gain stages. This requires the use of a small feedback capacitor in the preamplifier charge loop. In this case, a 0.5-pF feedback capacitor was adequate. When a small feedback capacitor is used, however, the open-loop bandwidth of the preamplifier must be as large as possible to retain a fast closed-loop rise time when relatively high input capacities are added to the preamplifier input.

In this case, the closed-loop bandwidth was maximized by using transistors having very high gain bandwidth and low capacity.

The preamplifier output response was measured using a Tektronix 454 oscilloscope having a 2.4-nsec rise time. An input pulse having a 5-nsec fall time (see Fig. 4A) was used for response measurements.

The measured output response was 9 nsec with zero external input capacitance (see Fig. 4B) and 15 nsec with 10-pF external input capacitance (see Fig. 4C). These rise-time figures are somewhat conservative since they include the rise-time contributions of the oscilloscope and the input pulse.

### PREAMPLIFIER CONSTRUCTION

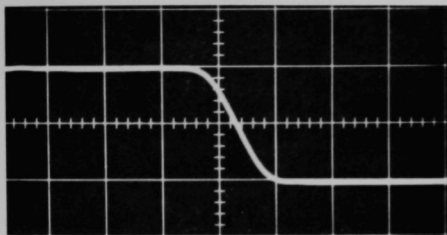
The preamplifier is built on a  $1\frac{3}{8} \times 4\frac{3}{4}$ -in. board, as shown in Fig. 5. All signal leads are short, particularly the lead connecting the collector of  $Q_3$  to the collector of  $Q_4$  and the base of  $Q_5$ , since any shunt capacity from this lead to ground reduces the open-loop bandwidth. The copper plating was left on the component side of the board, except around the input circuit, to act as a ground plane. The feedback and test capacitors ( $C_f$  and  $C_T$ ) are miniature piston trimming capacitors (Johanson type 7200, 0.1 to 1.3 pF), which allow precise gain adjustment.

Before being used in this preamplifier, the input FET ( $Q_1$ ) was selected for low noise in a test circuit.

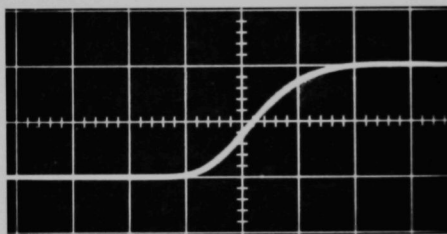
### CONNECTION TO THE PROPORTIONAL COUNTER

The proportional counter is insulated from ground, and the counter's bias voltage is applied at the cathode from a negative supply as shown in

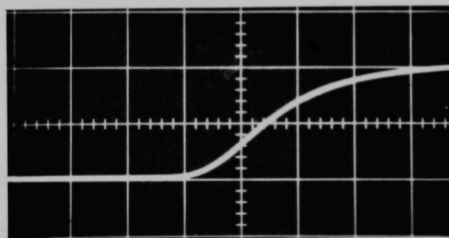




(A) Input Response. Vertical scale = 0.4 V/div and horizontal scale = 5 nsec/div.



(B) Output Pulse for Zero External Input Capacitance. Vertical scale = 0.2 V/div and horizontal scale = 5 nsec/div.

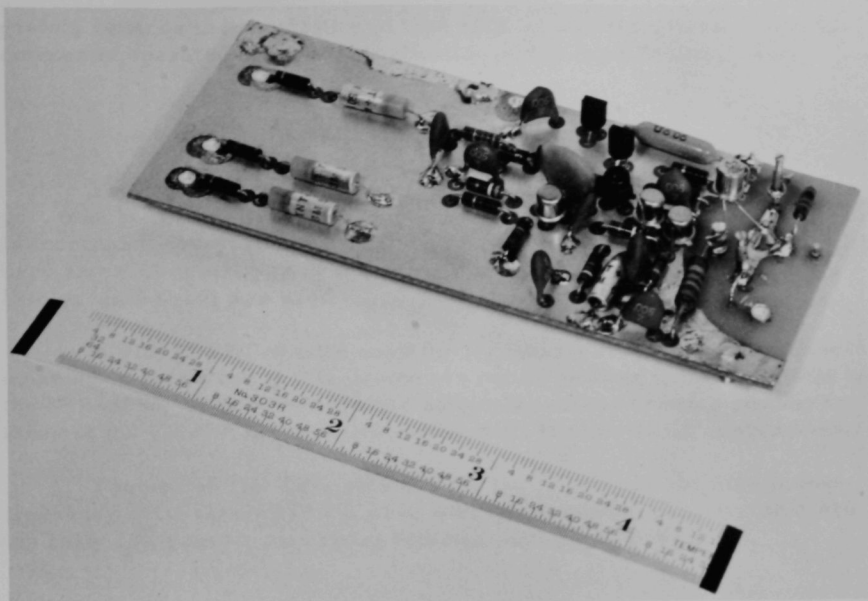


(C) Output Pulse for 10-pF External Input Capacitance. Vertical scale = 0.2 V/div and horizontal scale = 5 nsec/div.

ID-103-11924

Fig. 4. Preamplifier Response





ID-103-11862

Fig. 5. Photograph of Preamplifier

Fig. 1. This mode of operation differs from the conventional method (in which the cathode of the counter is grounded) and allows the preamplifier to be direct-coupled to the anode of the proportional counter, with the following advantages:

1. An isolation resistor at the anode of the counter is no longer required. The elimination of this resistor removes a source of noise.
2. A coupling capacitor between the anode of the counter and the input of the preamplifier is no longer required. The elimination of this capacitor decreases the stray capacity at the input of the preamplifier and improves the signal-to-noise ratio.
3. The input FET of the preamplifier is isolated by the proportional counter from the high-voltage bias supply. This isolation provides increased protection of the preamplifier's input FET against damage induced by transients on the high-voltage bias supply.
4. The bias voltage may be applied to the proportional counter through a low impedance at the counter's cathode. This type of connection



greatly reduces the possibility of bias shift across the counter when the counter is operated at high multiplication and at high counting rates.

### FURTHER APPLICATIONS

The low-frequency noise of the preamplifier described in this report may be further reduced if the resistance of the feedback resistor ( $R_f$ ) is increased. Typically, a 14% reduction in noise (for  $\tau = 2 \mu\text{sec}$  and with zero external capacity) has been obtained when a  $2 \times 10^9 \Omega$  resistor (Victoreen RX-25) was used.

A TIS-75 FET may be used for  $Q_1$ . However, the low-frequency noise characteristics of this device are not as good as those obtainable with the SFB-8558. (The SFB-8558 has electrical characteristics similar to those of the TIS-75, but is a new device built for low-noise applications.)

The use of TIS-75's (selected for low noise) has resulted in low-frequency noise figures ( $\tau = 2 \mu\text{sec}$  with zero external capacity) that are typically 25% greater than those obtained with the SFB-8558.





## APPENDIX

Overload Pulse Width

The width of  $T_1$  for the overload pulse (the width as measured from the leading edge of the peak of the pulse to a reference level,  $E_b$ ) from an amplitude-limiting amplifier having a gain  $A$  and an input  $E_1$ , as shown in Fig. 2B, may be determined as follows:

$$E_b = AE_p e^{-T_1/\tau_2}; \quad T_1 = \tau_2 \ln \frac{AE_p}{E_b}. \quad (A.1)$$

The width of the overload pulse from the same amplifier but with a saturated input  $E_2$ , as shown in Fig. 2C, may be determined as follows:

$$E_s = E_p e^{-T'/\tau_1}; \quad T' = \tau_1 \ln \frac{E_p}{E_s}. \quad (A.2)$$

The saturated level,  $E_s$ , decays to a new level,  $E_x$ , after passing through the pole zero correction network.  $E_x$  may be derived as follows:

$$E_x = E_s e^{-T'/\tau_2} + E_s \frac{R_2}{R_1 + R_2} - E_s \frac{R_2 e^{-T'/\tau_2}}{R_1 + R_2} \quad (A.3)$$

if

$$\tau_1 = R_1 C_1,$$

then

$$\tau_2 = \frac{R_1 R_2 C_1}{R_1 + R_2}$$

and

$$\frac{\tau_2}{\tau_1} = \frac{R_2}{R_1 + R_2}. \quad (A.4)$$

Substituting Eq. A.4 into Eq. A.3 gives

$$E_x = E_s \left( e^{-T'/\tau_2} + \frac{\tau_2}{\tau_1} - \frac{\tau_2}{\tau_1} e^{-T'/\tau_2} \right). \quad (A.5)$$

Since  $T' = \tau_1 \ln \frac{E_p}{E_s}$ ,



then

$$E_x = E_s \left[ \left( \frac{E_p}{E_s} \right)^{-\tau_1/\tau_2} - \frac{\tau_2}{\tau_1} \left( \frac{E_p}{E_s} \right)^{-\tau_1/\tau_2} + \frac{\tau_2}{\tau_1} \right]. \quad (A.6)$$

The time required for the pulse to decay from  $E_x$  to  $E_b$  is

$$T'' = \tau_2 \ln \frac{AE_x}{E_b}. \quad (A.7)$$

Substituting Eq. A.6 into Eq. A.7 gives

$$T'' = \tau_2 \ln \left\{ \frac{AE_s}{E_b} \left[ \left( \frac{E_p}{E_s} \right)^{-\tau_1/\tau_2} - \frac{\tau_2}{\tau_1} \left( \frac{E_p}{E_s} \right)^{-\tau_1/\tau_2} + \frac{\tau_2}{\tau_1} \right] \right\}.$$

The total width  $T_2$  of the overload pulse is

$$T_2 = T' + T'',$$

or

$$T_2 = \tau_1 \ln \frac{E_p}{E_s} + \tau_2 \ln \left\{ \frac{AE_s}{E_b} \left[ \left( \frac{E_p}{E_s} \right)^{-\tau_1/\tau_2} - \frac{\tau_2}{\tau_1} \left( \frac{E_p}{E_s} \right)^{-\tau_1/\tau_2} + \frac{\tau_2}{\tau_1} \right] \right\}. \quad (A.8)$$

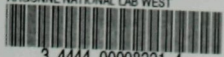


## REFERENCES

1. E. F. Bennett, Nucl. Sci. Eng. 27, (1967), 16-27.
2. C. H. Nowlin and J. L. Blankenship, Rev. Sci. Inst. 36 (1965), 1830.
3. A. B. Gillespie, *Signal, Noise and Resolution in Nuclear Counter Amplifiers*, Pergamon Press Ltd., London (1953).
4. T. V. Blalock, *Optimization of Semiconductor Preamplifiers for Use with Semiconductor Radiation Detectors*, ORNL-TM-1055 (Feb. 23, 1965).
5. A. Van der Ziel, Proc. IRE 50 (1962), 1808.



ARGONNE NATIONAL LAB WEST



3 4444 00008221 4

7

